

# Development of Reversed Shear Plasmas with Large Bootstrap Current Fraction towards Reactor Relevant Regime in JT-60U

Y. Sakamoto, G. Matsunaga, N. Oyama, T. Suzuki, N. Aiba, H. Takenaga, A. Isayama, K. Shinohara, M. Yoshida, M. Takechi, T. Fujita, S. Ide, Y. Koide, Y. Kamada and the JT-60 Team

Japan Atomic Energy Agency, Naka, Ibaraki-ken, 311-0193 Japan

e-mail contact of main author: sakamoto.yoshiteru@jaea.go.jp

**Abstract.** This paper reports the development of reversed magnetic shear (RS) plasmas with a large bootstrap current fraction ( $f_{BS}$ ) towards reactor relevant regime, especially lower  $q_{95}$  regime. By utilizing large volume configuration close to the conductive wall for wall stabilization, the beta limit of RS plasmas is significantly improved. As a result, high confinement RS plasmas with large  $f_{BS}$  exceeding no-wall beta limit are obtained in reactor relevant regime, where  $\beta_N \sim 2.7$ ,  $\beta_p \sim 2.3$  is achieved with reversed  $q$  profile with  $q_{min} \sim 2.4$ , and then  $HH_{98y2} \sim 1.7$ ,  $n_e/n_{GW} \sim 0.87$  and  $f_{BS} \sim 90\%$  are also obtained at  $q_{95} \sim 5.27$ .

## 1. Introduction

High beta, high confinement and large fraction of bootstrap current ( $f_{BS} > 70\%$ ) are required for DEMO reactor (Slim CS [1], SSTR [2]), where RS plasma with large bootstrap current driven in off-axis region is envisaged, because its current profile is naturally formed with the large  $f_{BS}$ . Large  $f_{BS}$  plasmas were reported from many tokamaks, especially in JT-60U a stationary RS plasma with  $f_{BS} \sim 75\%$  had been sustained for 7.4 s [3]. However the operational region is limited at high  $q_{95} > 8$  (safety factor at the 95% flux surface) in which  $f_{BS}$  is enhanced within the attainable beta limit without wall stabilization. Recently, the installation of ferritic steel tiles in JT-60U enable to produce the large volume plasma, close to the conductive wall for wall stabilization, with high NB heating power, and then a low plasma-rotation threshold for stabilization of the resistive-wall mode was identified [4]. Improved beta limit by wall stabilization can contribute to expanding the operational region in RS plasma with large  $f_{BS}$  to lower  $q_{95}$  regime.

## 2. RS plasma with large $f_{BS}$ in low $q_{95}$ regime

The experiments of RS plasma with large  $f_{BS} > 70\%$  were performed at high  $q_{95} > 8$  so far, due to lower beta limit typically imposed by  $\beta_N < 2$  in JT-60U RS plasmas without wall stabilization. The ideal MHD stability code (MARG2D) [5] indicates that ideal stability limit with ideal conductive wall is significantly improved when the plasma is close to conductive wall. For example,  $\beta_N > 3$  can be obtained with  $d/a \sim 1.2$ , where  $d$  is distance between plasma axis and conductive wall and  $a$  is plasma minor radius. In 2008 JT-60U experimental

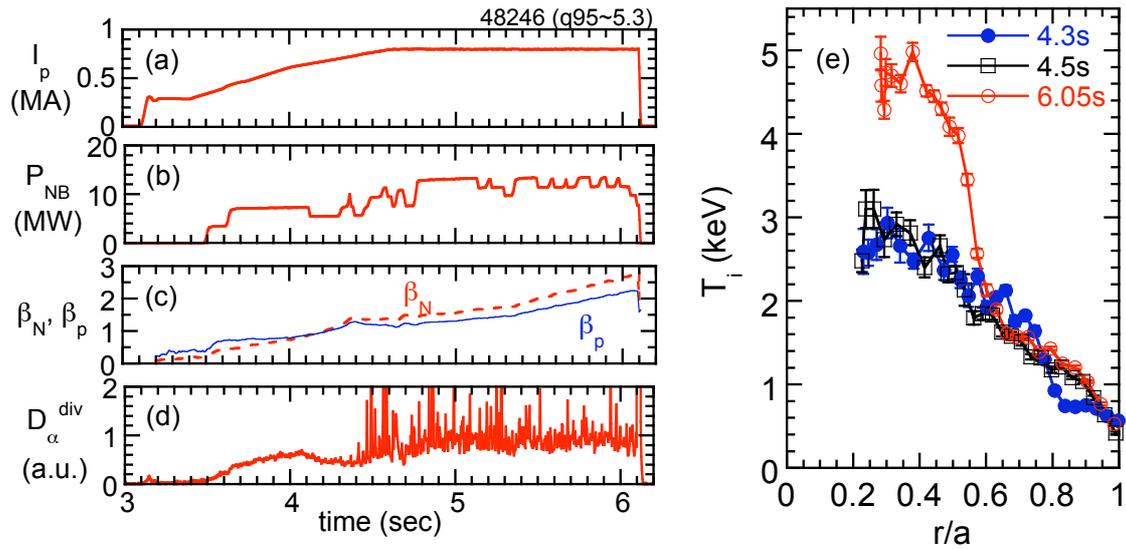


Figure 1. Typical waveforms of an RS discharge at  $q_{95} \sim 5.3$ . (a) Plasma current, (b) injected NB power, (c) normalized beta (dotted curve) and poloidal beta (solid curve), (d) deuterium recycling emission at the diverter. (e) Temporal evolution of ion temperature profile.

campaign, the RS plasma with large  $f_{BS}$  was emphasized in lower  $q_{95}$  regime by utilizing the large volume configuration ( $\sim 67\text{m}^3$ ) close to the conductive wall for wall stabilization. Previous stationary RS plasmas with large  $f_{BS}$  [3,6] was operated with high toroidal magnetic field of 3.4 T and plasma current of 0.8 MA resulting in  $q_{95} \sim 8.3$ . In this experiments, on the other hand, toroidal magnetic field was reduced up to 1.8T with keeping plasma current of 0.8MA, because the heating power is limited to attain high beta at high toroidal magnetic field.

Typical waveforms of the discharge are shown in Fig.1, where the plasma parameters are as follows: plasma current  $I_p = 0.8\text{MA}$ , toroidal magnetic field  $B_T = 2.0\text{T}$ ,  $q_{95} \sim 5.27$ , elongation  $\kappa \sim 1.5$ , triangularity  $\delta \sim 0.39$  and a ratio of the wall radius to the plasma minor radius  $d/a \sim 1.3$ . The value of  $q_{95}$  is actually close to DEMO reactor design. Since the effect of wall stabilization on the external kink mode with higher  $m$  number, where  $m$  is poloidal mode number, is weak at the fixed  $d/a$ , the stored energy feedback control was utilized to keep low beta in the ramp-up phase of plasma current. The ITB with wide radius ( $r/a \sim 0.8$ ) was produced before H-mode transition. Although the ITB was reduced after H-mode transition at  $t = 4.35\text{s}$ , the ITB was recovered with increasing beta during flat-top phase of plasma current, as shown in Fig. 1(e). Finally strong ITB was formed with the radius of 0.6. In this discharge,  $\beta_N \sim 2.7$  and  $\beta_p \sim 2.3$  were achieved, though the plasma was terminated by disruption at  $t \sim 6.1\text{s}$ . The achieved value of  $\beta_N$  is much higher than previous experiments of large  $f_{BS}$  plasmas with  $\beta_N \sim 1.7-2.2$  at  $d/a \sim 1.5$ . The disruption was caused by resistive wall mode ( $n=1$ ), of which growth time is the order of the resistive wall time ( $\tau_w \sim 10\text{ms}$ ) with decreasing toroidal rotation at  $q=3$  surfaces and it will be discussed later. The MARG2D code indicates that the plasma exceeds no-wall beta limit, where the beta limit with free boundary is  $\beta_N \sim 2.0$ . In addition high confinement enhancement factor over the L-mode scaling ( $H_{89}$ ) of  $\sim 2.9$  was

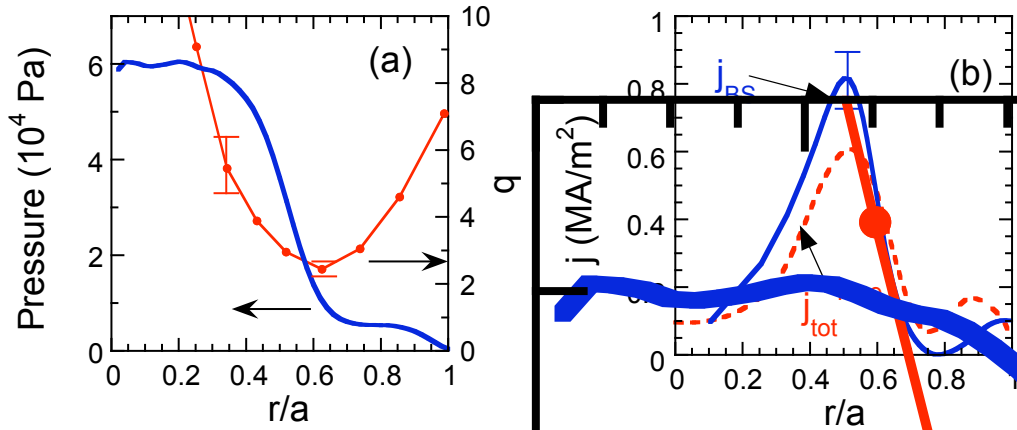


Figure 2. Radial profiles of (a) total pressure and safety factor, (b) measured total current density ( $j_{tot}^{mse}$ ) and the calculated bootstrap current density ( $j_{BS}$ ) at  $t \sim 6.05$ s.

obtained at high normalized density ( $n_e/n_{GW} \sim 0.87$ ) regime owing to both internal and edge transport barrier formation. Thanks to high density, the ratio of electron and ion temperature is  $T_e/T_i \sim 0.9$  at the center. Moreover high confinement enhancement factor over the ELMy H-mode scaling  $HH_{98y2} \sim 1.7$  was obtained owing to small contribution of beam component ( $W_{beam} \sim 0.46$  MJ) to total stored energy ( $W_{dia} \sim 2$  MJ). It is noted that  $dW_{dia}/dt \sim 1$  MW is considered in the calculation of energy confinement time due to transient phase. Reversed  $q$ -profile was formed with  $q_{min} \sim 2.4$  and its location  $\rho_{q_{min}} \sim 0.6$  just before disruption, and the ITB foot located around there, as shown in Fig. 2(a). Radial profiles of total current density measured with MSE diagnostic and the calculated bootstrap current evaluated from ACCOME code at the end of discharge are shown in Figure 2(b). The calculated bootstrap current, especially in ITB region, exceeds measured total current density due to the transient nature, which shows the current profile does not reach steady state condition. However temporal evolution of  $q_{min}$  and  $\rho_{q_{min}}$  shows the current profile is approaching fixed value. Therefore the current profile is not far from steady state solution and it will be discussed later. The  $f_{BS} \sim 90\%$  is achieved at the end of the discharge. Since one unit of CO-NB and one unit of CTR-NB were injected, namely balanced injection, beam driven current is negligible in the discharge.

Figure 3 shows typical waveforms of the discharge with  $q_{95} \sim 6.1$ , where toroidal magnetic field is 2.24. In this discharge, NNB power of 3.3 MW and LH power of 0.68 MW was injected from  $t = 5.8$  s. Then  $\beta_N \sim 2.75$  and  $\beta_p \sim 2.53$  were achieved, though the plasma was terminated by disruption at  $t \sim 6.15$  s. One of the most interesting features is disappearance of ELM activity. Actually H-mode transition was occurred at  $t = 4.75$  s where ion temperature starts to increase at edge region. The Broadband fluctuation only

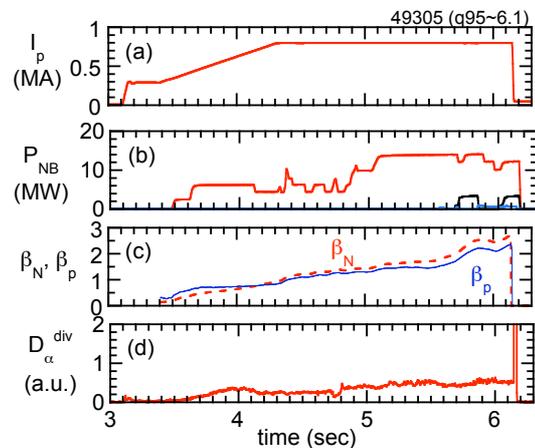


Figure 3. Typical waveforms of an RS discharge at  $q_{95} \sim 6.1$ , similar to Fig. 1.

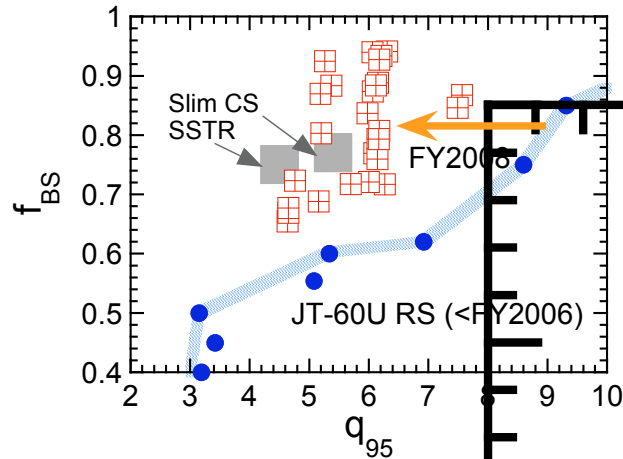


Figure 4. Expanded operational regime towards large  $f_{BS}$  and lower  $q_{95}$  in JT-60U RS plasmas together with DEMO reactor.

at peripheral region was observed in ECE signal during no ELM period after H-mode transition. This edge fluctuation might affect edge pressure profile to suppress ELM activity, like QH-mode. Thanks to no ELM activity, ITB radius in  $q_{95} \sim 6.1$  regime tends to wider than that in  $q_{95} \sim 5.3$ .

Figure 4 shows the progress of large  $f_{BS}$  towards lower  $q_{95}$  regime for the RS discharges in JT-60U together with DEMO reactor (SSTR and Slim CS). It is obvious that the reactor relevant large  $f_{BS}$  has significantly expanded towards low  $q_{95}$  regime. Furthermore, the achieved parameters, including  $\beta_N$ ,  $f_{BS}$ ,  $HH_{y2}$ ,  $n_e/n_{GW}$ ,  $q_{95}$  and  $q_{min}$ , are very close to or exceed ITER steady-state scenario (VI) [7].

### 3. Transport analysis and confinement property

For the steady-state operation of tokamak, the plasma current must be driven by non-inductive current drive. From the viewpoint of tokamak reactor design, the large fraction of bootstrap current, driven by the high  $\beta$  plasma itself, to plasma current is required for reducing a circulating power for non-inductive current drivers, which is typically above 75%. Since an ITB contributes to enhance bootstrap current, optimization of ITB is one of the key factors to produce large  $f_{BS}$  plasmas. In addition, the reversed magnetic shear configuration helps to produce strong ITB and is naturally formed with a large  $f_{BS}$ . In JT-60U, ITBs were formed during ramp-up phase of plasma current with NB heating. Early NB heating delays the penetration of inductive current and the formation of ITB makes the penetration delay further. As the results, wide ITB radius could be produced. Then beta was increased with increasing NB power.

Figure 5 shows radial profiles of typical large  $f_{BS}$  plasma with  $q_{95} \sim 6.1$  shown in Fig. 3. The ITB structure with steep gradient is clearly seen in the ion temperature, electron temperature and electron density profiles. Wide radius of ITB was formed, which is located around  $\rho_{qmin}$ ,

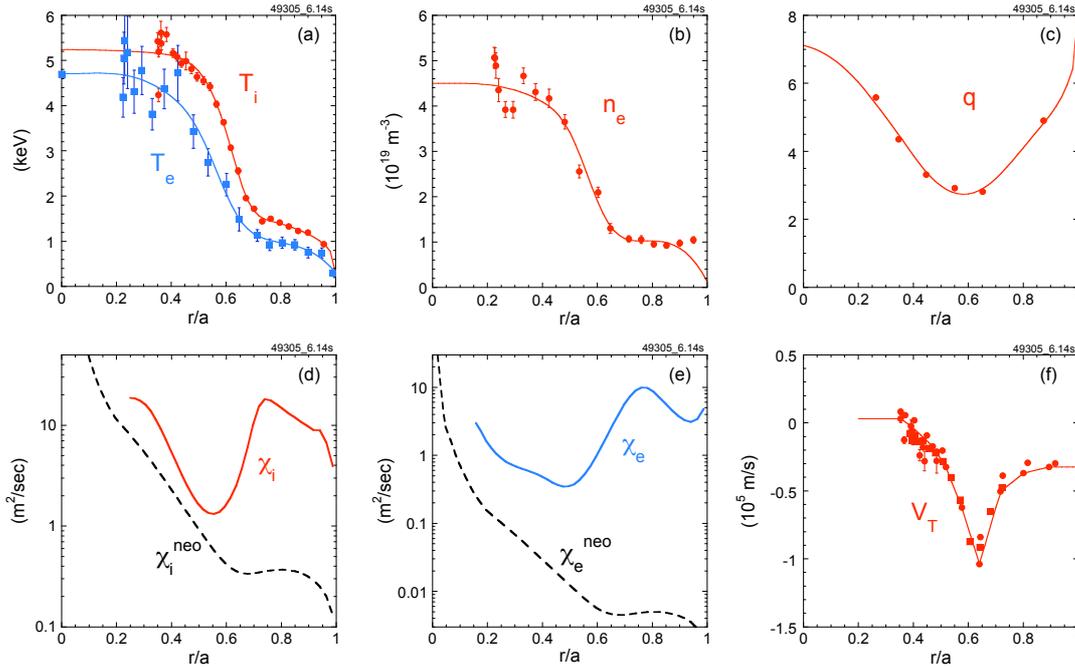


Figure 5. Radial profiles of (a) ion and electron temperatures, (b) electron density, (c) safety factor, (d) ion thermal diffusivity and neo-classical prediction, (e) electron thermal diffusivity and neo-classical prediction, (f) toroidal rotation velocity for the discharge shown in Fig. 3.

as shown in the figure. The notch structure is seen in toroidal rotation profile, which is usually observed in JT-60U RS plasmas with strong ITB even with balanced NB injection [8]. The thermal diffusivity profiles evaluated using TOPICS code illustrate the ITB characteristics. The ion thermal diffusivity decreases around step gradient region of ion temperature and approaches neoclassical predicted level. The thermal diffusivity for electron is similar to that for ion, however its level is much higher than neoclassical prediction.

In 2008 campaign, the value of  $q_{95}$  was varied in the range from 4.6 to 6.3 by changing toroidal magnetic field with fixed plasma current of 0.8MA. In Fig. 6(a),  $HH_{y2}$  factor is

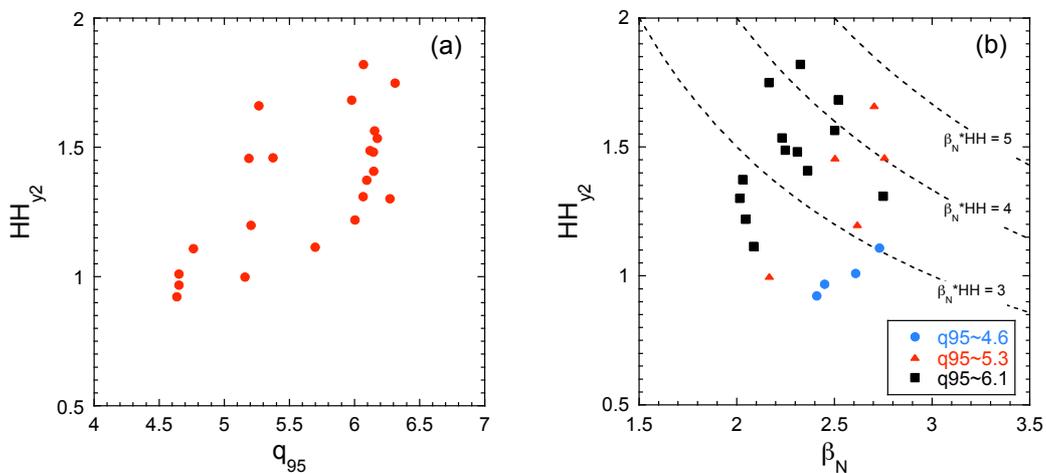


Figure 6.  $HH_{y2}$  factor as a function of (a) safety factor at the 95% flux surface  $q_{95}$  and (b) normalized beta  $\beta_N$ .

plotted against  $q_{95}$ . The  $HH_{y2}$  factor roughly increases with increasing  $q_{95}$ . The  $HH_{y2}$  factor is low especially in  $q_{95} \sim 4.6$  region. In this region, H-mode transition was occurred early due to lower toroidal magnetic field. This causes the reduction of ITB in early phase, and then reversed magnetic shear  $q$ -profile become weaker, and ITB strength become also weaker, which leads lower confinement. The higher  $HH_{y2}$  in  $q_{95} \sim 6.2$  may be due to disappearance of ELM activities as described in Sec. 2. In Fig. 6(b),  $HH_{y2}$  factor is plotted against  $\beta_N$ . The product of  $\beta_N HH_{y2}$  exceeds 4 in several discharges with  $q_{95} = 5.1-6.3$ . In case of data with  $q_{95} \sim 4.6$ ,  $\beta_N$  increases linearly with increasing  $HH_{y2}$  due to the limitation of heating power.

#### 4. Stability of large $f_{BS}$ plasma with wall stabilization

Since the operation region of large  $f_{BS}$  plasma limited in high  $q_{95}$  region so far is due to lower beta limit of RS plasma, the key role of improvement of beta limit is stabilization of kink-ballooning mode by conducting wall. By improving beta limit, operation region of large  $f_{BS}$  plasma can be expanded into reactor relevant  $q_{95}$  region. Figure 7(a) shows the achieved  $\beta_N$  is plotted against  $d/a$  for the large  $f_{BS} > 70\%$  plasmas. Previous large  $f_{BS}$  plasmas were operated with  $d/a > \sim 1.5$  and sustained  $\beta_N$  was less than  $\sim 2.1$ . The ideal MHD stability code (MARG2D) indicates that ideal stability limit will be improved by the ideal conductive wall as  $d/a < 1.4$ , and then  $\beta_N > 3$  can be obtained with  $d/a \sim 1.2$ . Therefore, plasma configuration was optimized with  $d/a \sim 1.3$  for  $q_{95} = 4.6-5.3$ ,  $\sim 1.2$  for  $q_{95} \sim 6.1$  in 2008 campaign. The achieved  $\beta_N$  was significantly enhanced with smaller  $d/a$ , as shown in the figure. It seems that there is an upper limit in  $\beta_N$  of 2.8. Although  $\beta_N$  increases with decreasing  $q_{min}$  as shown in Fig. 7(b), there is an upper limit in  $\beta_N$ . The MARG2D code indicates that the ideal wall beta limit is  $\beta_N \sim 3.0$  and the free boundary beta limit is  $\sim 1.65$ , resulting  $C_\beta \sim 0.85$ , for the discharge shown in Fig. 3 and Fig. 5. Therefore the upper limit in  $\beta_N$  is close to the ideal wall beta limit.

The discharges were terminated in disruption, where slowly growing MHD mode ( $n=1$ ) such

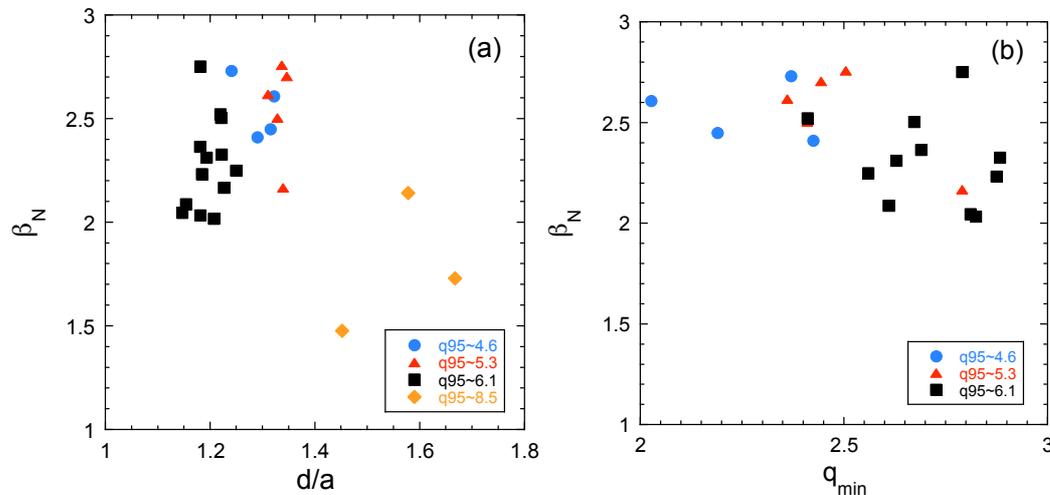


Figure 7. Normalized beta  $\beta_N$  as a function of (a) the ratio of wall radius to minor radius and minimum value of safety factor.

as RWM was observed just before disruption, as shown in Fig. 8(d). The temporal evolution of  $q_{\min}$  and  $\rho_{q_{\min}}$  together with location of  $q=3$  surfaces ( $\rho_{q=3}$ ) are shown in Fig. 8(a) and 8(b). The value of  $q_{\min}$  decreases in time and approaches fixed value, while  $\rho_{q_{\min}}$  keeps almost same location after  $t=5$ sec in the discharge. In RS plasma with  $q_{\min} < 3$ , there are two  $q=3$  surface. Outer  $q=3$  surface moves outward and inner  $q=3$  surface inward with decreasing  $q_{\min}$ . Recent experiments identified that a low toroidal rotation threshold for stabilizing RWM, where the toroidal rotation velocity at the low order rational surface plays important role [4,9]. The temporal evolution of toroidal rotation velocities at  $\rho_{q_{\min}}$  and  $\rho_{q=3}$  are shown in Fig. 8(c). Since the toroidal rotation at  $\rho_{q_{\min}}$  locates around the notch in the profile, that increases in ctr-direction with growing ITB. On the other hand, toroidal rotation at both  $q=3$  surfaces decreases, because  $q=3$  surfaces move inward and outward on toroidal rotation profile with notch structure. Therefore, it can be considered that the slowdown of toroidal rotation velocity at  $q=3$  surfaces caused the destabilization of RWM in the discharge. Figure 9 shows the radial displacements of  $n=1$  kink-ballooning mode calculated by MARG2D code with free boundary condition, together with  $q$  profile measured with MSE diagnostic. This eigen-function has the dominant  $m=3$  component which is excited in between  $q=3$  surfaces.

#### 4. Summary

Recent progress in RS plasma with large  $f_{BS}$  has been made towards reactor relevant regime, especially lower  $q_{95}$ . By utilizing large volume configuration close to the conductive wall for

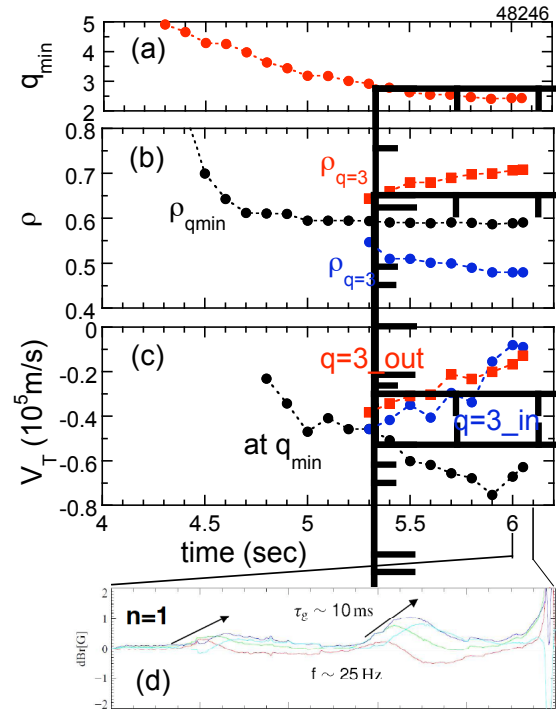


Figure 8. Temporal evolution of (a)  $q_{\min}$ , (b) location of  $q_{\min}$  and  $q=3$  surfaces, (c) toroidal rotation velocity at the positions of  $q_{\min}$  and  $q=3$ . (d) Magnetic perturbation ( $n=1$ ) measured by saddle loop coils, just before disruption.

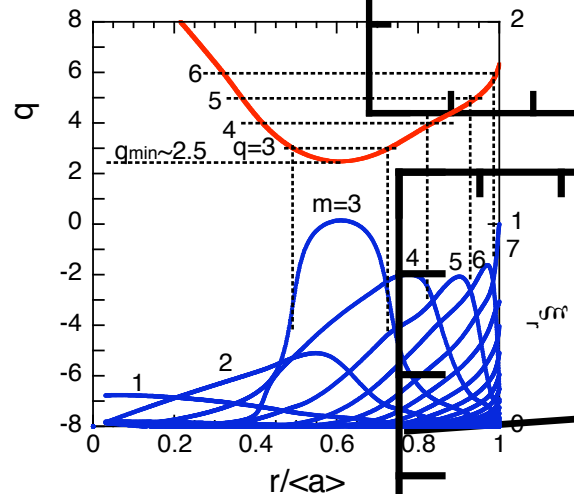


Figure 9. Safety factor profile and the radial displacements of  $n=1$  kink-ballooning mode calculated by MARG2D with free boundary condition.

wall stabilization, beta limit is significantly improved. As a result, high confinement RS plasmas exceeding non-wall beta limit with large  $f_{BS}$  are obtained in reactor relevant regime in JT-60U, where  $\beta_N \sim 2.7$ ,  $\beta_p \sim 2.3$  is achieved in RS plasma with  $q_{min} \sim 2.4$ , and then  $HH_{98y2} \sim 1.7$ ,  $n_e/n_{GW} \sim 0.87$  and  $f_{BS} \sim 90\%$  are obtained at  $q_{95} \sim 5.27$ . The MARG2D code indicates that the ideal wall beta limit is  $\beta_N \sim 3.0$  and the free boundary beta limit is  $\sim 1.65$ , resulting  $C_\beta \sim 0.85$ . The achieved parameters, including  $\beta_N$ ,  $f_{BS}$ ,  $HH_{y2}$ ,  $n_e/n_{GW}$ ,  $q_{95}$  and  $q_{min}$ , are very close to or exceed ITER steady-state scenario (VI). The discharges were terminated in disruption, where slowly growing MHD mode ( $n=1$ ) such as RWM was observed. It can be considered that the slowdown of toroidal rotation velocity at  $q=3$  surfaces caused the destabilization of RWM.

### Acknowledgements

The authors would like to acknowledge the members of the Japan Atomic Energy Agency who have contributed to the JT-60U projects.

### References

- [1] TOBITA, K., et al., Nucl. Fusion **47** (2007) 892.
- [2] KIKUCHI, M., Nucl. Fusion **30** (1990) 265.
- [3] SAKAMOTO, Y., et al., Nucl. Fusion **45** (2005) 574.
- [4] TAKECHI, M., et al., Phys. Rev. Lett. **98** (2007) 055002.
- [5] TOKUDA, S. and WATANABE, T., J. Plasma Fusion Res. **73** (1997) 1141.
- [6] SAKAMOTO, Y., et al., Nucl. Fusion **47** (2007) 1506.
- [7] Plasma Performance Assessment 2004 section 3.4, ITER Technical Basis ITER EDA Documentation Series.
- [8] SAKAMOTO, Y., et al., Nucl. Fusion **41** (2001) 865.
- [9] REIMERDES, H., et al., Phys. Rev. Lett. **98** (2007) 055001.